The application of centrifuge models in the study of an interaction problem

M.D.BOLTON & K.W.MAK *Cambridge University, UK*

1. Introduction

The problem of a shallow strip footing resting on sand which is supported by a neighbouring L-shaped retaining wall will be considered (figure 1). The main objects of design of such a system are firstly to avoid collapse, and secondly to ensure serviceability. Moreover, unless the correct mode of failure of the soil-structure system is ascertained, effort devoted to choosing the design parameters and predicting deformation would be futile (Bolton, 1981). Therefore, establishing the correct mode of failure must be the logical first step in tackling the present problem. Three limit states of the system are possible. The deflection of the wall can lead to extra settlement of the footing when it is loaded; the extra earth pressures can lead to structural problems for the wall; and the footing/wall complex can indulge in a composite failure.

The cost and time involved in the observation of collapse modes by means of full scale experiments tend to limit the variety of tests possible. Also, it is difficult to control the environment of a full scale test. By comparison, the centrifuge method is powerful, effective and cheap (Schofield, 1980 and 1981). The centrifuge tests performed for this work will be regarded as independent geotechnical events with careful control of ground conditions.

Only rigid retaining walls will be considered: structural failure of the wall is beyond the scope of this paper. Both the backfill and the soil supporting the foundation of the model wall have been made of a single dry granular soil. Attention will be limited to one grain

size. One particular strip footing will be considered, its width being expected to lead to failures of the footing either alone or in conjunction with the retaining wall. Three parameters will be examined: the density of the sand, the distance of the footing from the wall and the width of the base of the wall.

2. Apparatus and Instrumentation

The Cambridge Geotechnical Centrifuge has been described by Schofield (1980). The model was built in a strong box (Mak, 1983b), the front face of which consisted of a removable 80 mm thick perspex sheet. A 50 mm gap was left above the back of the box to allow access to the soil model after the front window had been closed (figure 2).

The retaining wall (figure 3) used in all but one of the tests was made up of dural blocks so that, by varying the number of blocks in the assembly, both the height of the wall and the width of the base could be changed. These dural units were accurately located by dowels and were held together by bolts. Each carried one or more contact stress transducers. A maximum of four contact stress transducers could be carried on the stem of the wall and four, on the base. In a typical arrangement, there were two columns of transducers, one on the back of the wall and another on the base. However, built-in symmetry of the blocks would allow turning the base units upside down so that the contact stress transducers faced the top surface of the base. A circular diaphragm type load cell was also incorporated into the end plate at the heel of the wall. In addition, two shaped foam rubber skirts were clamped one to each edge of the wall. These skirts served to prevent any sand grains from getting trapped between the model wall and the strong box containing the experiment. This model wall was to be used at 60 g. In order to establish the internal consistency of the experiments (Schofield, 1980), it was decided to repeat one of the tests at 105 g. The model wall used at 105 g was a 60/105th model of its 60 g counterpart and was made up of plane dural sections welded together, with no contact stress transducers.

The contact stress transducers were similar to the ones described by Stroud (1971). An exploded view of the transducer is shown in figure 4. The active face A was screwed to the rigid top block B, which was, in turn, connected by thin metal webs (a, b, c) to the base block (C) of the transducer. The transducer was designed to measure the normal force, the shear force and the eccentricity of the normal force acting on its active face. The normal force was carried almost entirely by compression in the 4 vertical webs, the horizontal webs offering little resistance. Similarly, the shear force was carried mainly by tension in one pair of horizontal webs (c) and by compression in the other. Foil gauges were used to measure the strains in the webs. These gauges were wired into three Wheatstone bridge circuits, one to measure the strains in the shear webs and one to measure the strains in the pair of normal webs at each end of the transducer. It is assumed that the direction of the applied shear stress is coincident with the direction of the shear webs and that the eccentricity of the normal stress will only be in the line of the shear webs.

The method of calibration preferred at Cambridge was suggested by Hambly (1969) and has been described by many others (Stroud, 1971 and Bransby, 1973). It has long been recognised that a solitary load cell stiffer than its surrounding soil will over-register, and a boundary cell softer than the soil will under-register (Weiler & Kulhawy, 1982). In this work, the load cells were made as stiff as practical. The likely extent of under-registration was demonstrated by embedding the transducers, mounted in their wall units, underneath a 45 mm thick bed of sand. A medium coarse sand identical to that used in the main tests was employed. A uniform pressure was applied on the surface of the sand bed by means of an inflatable rubber diaphragm. The under-registration and hysteresis of the load cell response were found to be tolerable. Indeed, since any attempt to correct the under-registration of the load cells would require knowledge of the soil stiffness at any one stage of an experiment, it was considered impractical. It was, therefore, decided not to tamper with the raw measurements. Provided that the extent of under-registration was more or less uniform for all the transducers, the earth pressure profile constructed from raw stress data should be useful qualitatively, if not perfect in detail. Finally, the model wall had to be mounted in the centrifuge in the

manner in which it was to be used. The effect of enhanced gravity on the self weights of different components of the load cells could, thus, be measured and allowed for in subsequent calculations.

A strip load may be free to move with the retaining wall or it may be restrained, for example, by other parts of the structure. In this work, the strip load was allowed to rotate and translate with the backfill. The loader was a purpose-built jack (figure 5). The load was transmitted through a knife edge on the footing so that the footing was free to rotate. At the same time, the jack was supported on a wide rail with rollers in such a way that the whole assembly worked rather like a monorail vehicle and was free to translate. Milled on the piston of the jack was a taper, against which rested a perspex rod. As the footing settled and the piston moved out, the taper pushed the rod away from the jack. The rod, in turn, deflected a strain-gauged cantilever, thus giving a direct measure of the settlement. The piston was prevented from being blown out of its casing by a number of shear pins. The rail was fixed on the inner roof of the strong box.

Two similar strip footings were available, one 40 mm wide and the other, 22.9 mm wide, the ratio between their dimensions being 1.75 to 1. The former was to be used at 60 g; the latter, 105 g.

The general arrangement of the pressure system feeding the loader can be seen in figure 6. The pressure source was a pair of nitrogen cylinders mounted near the axis of the centrifuge. These cylinders were linked to a pressure regulating system by a flexible hose and copper tubing. The pressure regulating system was housed in a dural trough bolted on the swinging platform of the centrifuge. The accumulator consisted of two chambers separated by a diaphragm. One of these chambers, together with the loader and the connecting hose, was filled with a light hydraulic oil, air being carefully flushed out. The other chamber, the nitrogen cylinders, the copper tubing and the connecting hose were filled with compressed nitrogen. The flow of nitrogen was controlled by two normally closed solenoid valves while the flow of oil was controlled by a needle valve and a solenoid valve.

After the nitrogen cylinders had been charged, the gas compartment of the accumulator could be pressurised by opening solenoid valve A with valve B closed or vented by opening valve B with valve A closed. The nitrogen pressure built up in the accumulator could, in turn, be used to pressurise the loader by opening valve C momentarily. Switching for valve C was executed by means of an electronic timer with a resolution of 0.1 second although the actual switching time was probably controlled by the inertia of the moving parts of the valve. The main function of the accumulator was to connect a pneumatic system to a hydraulic system.

A hydraulic loader was preferred because it would allow observation of falling-load characteristics that would be expected, say, after brittle failures. Compressed nitrogen, on the other hand, represented a convenient means of providing high pressure in flight. The resolution of the loading increment achieved was better than 10 kg against a maximum load of 2 tonnes. The applied load was deduced by monitoring the pressure in the loading system.

The rigid body movement of the model wall was monitored with two horizontal and one vertical LVDTs. A standard nickel-chromium thermocouple was stuck to the face of the model wall to detect any temperature drifts in the transducer signals. Up to 30 channels of signals could be logged in quick succession on paper tape. Alternatively a magnetic tape recorder could be used to monitor up to 14 channels simultaneously when fast events were anticipated. Unfortunately, the two systems could not be used at the same time because of interference.

Embedded in the model soil construction was a matrix of silver ball markers visible through the perspex side of the strong box (figure 7). Thus, the development of strains in the soil mass could be recorded and deduced from photographs taken from behind an observation hatch through the roof of the centrifuge chamber. Polaroid film was used to provide instant information during a test while 70 mm film was reserved for quantitative interpretation after the test. In addition to the silver balls, the cross-section of the soil model next to the perspex window was either covered with a thin coat of brittle paint or stripes of coloured sand, thus aiding visual appreciation of the

failure mechanism. This could be studied on a TV monitor during a test or more carefully afterwards.

3. The Experiments

The strong box was supported with its back plate horizontal and the geometry of the model construction was set out with the help of removable aluminium formers. Leighton Buzzard 14/25 sand (Stroud, 1971) was poured, parallel to the axis of the model wall, from a conical hopper suspended from an overhead crane. The height of drop and the rate of pouring were controlled to produce the required density of the soil (James, 1965). When sand pouring had been completed, a vacuum cleaner was used to level the surface of the model. Stripes of coloured sand were then sprinkled on the sand surface. Alternatively, the sand surface was sprayed with a thin film of paint. It was important to check that the paint had dried before proceeding further. Next, a regular matrix of silver balls was placed with the help of a perspex template and the spacing of the balls adopted was 15 mm. After the perspex window had been closed, the strong box was turned upright through 90° with a crane. The movement of the model wall incurred during the manipulation was found to be negligible. Finally, the formers were removed, the LVDTs were mounted and the strong box was loaded onto the centrifuge.

Typically, the centrifuge was brought up to the test rotational speed at 10 g intervals, readings being taken at each interval. Two reference 70 mm photographs were taken at 10 g. Subsequently one or two photographs were taken after every centrifuge speed increment. At the test centrifuge acceleration, the inlet valve to the accumulator was turned on for 0.1 seconds while keeping the vent closed. The pressure so built up in the accumulator was then divided into, generally, two to three load increments by manually energising, for short durations, the solenoid valve (C) that controlled the flow of the oil in the loader. The strip footing was loaded to failure or until the capacity of the loader was exhausted. A failure was detected either as a drop of the load that the wall could support or gross movements of the wall or the footing. Usually, loading would be continued a little beyond the failure to allow observation of the post-peak behaviour of the wall.

4. Results

Test C2 (figure 7) exhibited most of the typical features of the experiments performed (Mak, 1983a & b). The additional rigid body movements of the model wall and the footing due to the applied strip load are shown in figure 8, the movements incurred during acceleration of the centrifuge to the test speed (60 g) having been excluded. The movements of the wall were calculated from LVDT data.

The strain field observed in test C2 one load increment after the peak strip load is shown in figure 9. It can be seen that the displacement was concentrated in a small area behind the retaining wall and below the footing (figure 9a). Bands of high principal strain (figure 9b) have been delineated to identify possible locations of rupture bands. Local pockets of high principal strain judged to be the result of obvious errors in the estimated silver ball displacements were ignored in the determination of such locations. These notional rupture bands, when transferred to the displacement map, seemed to be consistent with the discontinuities in the displacement field. In figure 9c, the shear strains at the locations of the markers have been contoured by hand. Again, zones of concentrated strains, similar to the notional rupture bands, were evident.

Photographs of the model before and after the test are shown in plates 1 and 2. Typically, the failure mechanism consisted of two rupture bands, one running from the leading edge of the footing to the upper edge of the heel of the wall and the other running from the trailing edge of the footing to the lower edge of the heel of the wall. The former was slightly concave downward while the latter, concave upward. In front of the toe of the retaining wall, there was a small heap of soil suggesting that the toe had either failed in bearing or had ploughed into the soil as it moved forward. Behind the heel was a small void left behind by the advancing base of the wall. Superimposing successive photographs of the model confirmed that the footing, together with the loader, moved forward with the retaining wall during the test.

The stress envelope surrounding the model wall could be developed using load cell data (figure 10). On the top and posterior surfaces of the base where Stroud cells were not available, the normal pressure was measured with total load cells and the shear stress was taken as zero. The Stroud cells were 33.3 mm wide and were located at the centre of the model. Thus, the stress profile nominally referred only to this central strip. However, the diaphragms of the total load cells were only 21 mm in diameter although they were also located near the centre of the model. Three loading cases were considered: no load, peak applied strip load and one load increment beyond the peak load. The difference between the stresses corresponding to the maximum load and those recorded before a strip load was applied represented the additional stresses induced by the peak strip load. The maximum increase in normal stress seemed to occur between the bottom and the lower third point of the stem. The applied load also had the effect of increasing the bearing pressure near the toe and decreasing that near the heel. The most significant feature of failure seemed to be the lowering of the line of action of the normal stress acting on the stem. Also, the bearing pressure changed. This drop in the bearing pressure near the toe suggested that either the moment tending to topple the wall was reduced or the soil underneath the toe softened.

Consider figure 11. The stress profile surrounding the central strip of the retaining wall could be condensed into a polygon of three forces: the self-weight of the central strip of the wall (KI), the resultant of the forces acting on the base (IJ) and the resultant of the forces acting on the remaining surfaces (JK). Such a polygon of force was calculated for test C2 using simple statics (figure 12). The force polygon very nearly close, showing the high overall quality of the stress measurements and the acceptability of the assumptions made. The line of action of the force JI is shown in figure 13 while that of the force JK, in figure 14. The force JI represents the sum of the force JK and the weight of the central strip of the wall (KI).

Figure 15 compares the wall movements observed in tests with the same geometry as test C2 but different soil densities. All tests considered, except test C4, were conducted at 60 g. Test C4 was a model of test C1 and was carried out at 105g(Schofield, 1980). The settlement of the footing in these tests, except C4, is shown in figure 17. The effect of changing the density of the soil on the peak applied strip load can be seen in figure 16. From strain data and observations, it was found that the failure mechanism in these tests was independent of the density of the soil. This can be compared, say, with the split plane in a direct shear box test. This plane, dictated by the geometry of the shear box, is independent of the material being tested.

5. Discussion

If the collapse of the centrifuge model coincided with the failure of the foundation of the model wall, a formula predicting the bearing capacity of a strip footing could be used to back analyse the angle of shearing resistance mobilised in the model at collapse. Naturally, if the assumption was wrong, the back analysis would be meaningless. In such cases, hopefully, some anomalies would emerge to allow these meaningless back analyses to be spotted and eliminated. Meyerhof's footing formula (1953) has been adopted as follows:

$$q_{ult} = \tfrac{1}{2}\left(1 - \frac{\delta}{\phi}\right)^2 N_\gamma B' n \gamma + \left(1 - \frac{\delta}{90^\circ}\right)^2 N_q n \gamma D_0$$

where

q_{ult} = ultimate bearing capacity,

δ = angle of friction mobilised on the base,

ϕ = angle of shearing resistance,

B = width of the base,

e_b = eccentricity of the resultant normal force acting on the base,

B' = effective width of the footing $(B - 2e_b)$,

$N_q = \tan^2\left(45^\circ + \frac{\phi}{2}\right) \exp(\pi \tan\phi)$,

$N_\gamma \simeq 1.8 \tan\phi\, N_q$ (Hansen, 1961),

n = number of gravities (due to the centrifuge),

γ = unit weight of the soil, and

D_0 = depth of overburden.

For a given test, ϕ was the only unknown and could easily be back-calculated. The results were compared with the values of ϕ obtained

for standard laboratory shear tests (figure 18). The back analysed ϕ of test C1 fell below what would be expected from the laboratory tests, it was thought, because the maximum angle of base friction δ was exceeded. The rigid body displacement of the model wall seemed to support the hypothesis of a sliding failure in test C1 (figure 15).

The coefficient of lateral earth pressure at different heights on the stem of the wall could be calculated from the Stroud cell data. Before a strip load was applied, the coefficient was found to increase downward along the stem. The average coefficient of lateral earth pressure, K_{av}, was obtained by dividing the total horizontal force acting on the Stroud cells in the stem by $\frac{1}{2} W_{cs} \rho_s g H_s^2$ where ρ_s is the density of the soil, H_s is the height of the stem and W_{cs} is the width of the Stroud cell. During the acceleration of the centrifuge, K_{av} was found to decrease with increasing outward displacement of the model wall. In addition, if the maximum of such values of K_{av} was taken to be the coefficient of lateral earth pressure at rest, Ko, it was possible to estimate the angle of shearing resistance at low stresses using Jaky's relationship (Wroth, 1975). The results compared very well with the triaxial ϕ measured using σ_3 = 30 kPa (Mak, 1973b). Direct shear ϕ at this stress level was not measured.

The idealised failure mechanism can be broken up into free bodies as shown in figure 19. The normal and shear forces acting on the base of the wall, N_B and S_B respectively, were calculated as the sum of IK and KJ from the polygon of measured forces acting on the model wall (figure 11). This sum was, to a large extent, made up of the weight of the wall, which was immune from under-registration. Thus, it was thought to give a better estimate of the forces N_B and S_B, than calculating the forces directly from load cell data. It should be recalled that all the direct force measurements, with the notable exception of the strip load, Q, were made in a narrow central strip. Thus, Q had to be corrected for side friction before it became compatible with the other forces required to define the free body diagrams. An empirical procedure was employed. It was assumed, at failure, that the side friction affecting the magnitude of the effective strip load was generated only on the sides of the triangular failure wedge CDE (figure 19a), and that the pressure due to the strip load spread at a slope of 2:1.

The coefficient of lateral earth pressure at rest was taken as relevant and the coefficient of friction between the soil and perspex was measured in a direct shear box. In order to estimate the magnitude of side friction, the vertical pressure due to the strip load was calculated at seven evenly spaced depths and the resultant friction was deduced numerically, the resultant being assumed to point along the inclined plane II.

Since the weights and forces acting on the blocks of soil adjoining the vertical plane VV could be clearly deduced, this plane seemed the ideal site for exploring the pattern of interaction between the soil, the structure and the applied strip load. In figure 20, the average ϕ mobilised in the plane VV was plotted against the settlement of the footing up to the maximum load. ϕ is seen to increase continuously with increasing settlement of the footing, the maximum value of ϕ occurring at the peak applied strip load. In figure 21, the average ϕ mobilised on the inclined plane II was plotted against the settlement of the footing. The peak ϕ mobilised on the planes VV and II compared very well with those measured in the direct shear box (figure 22). It is interesting that it took less settlement of the footing to mobilise the first peak of ϕ on the plane II than on the plane VV. This seemed consistent with the strain data which showed that, for a given settlement, the shear strains were higher along plane II than along plane VV.

Therefore, the shear strains set up by the applied strip load seemed to concentrate along planes VV and II. Indeed, the strains on plane VV must have been important in transferring the load to the retaining wall. However, the mobilisation of the peak ϕ on these surfaces did not necessarily induce immediate failure of the wall. The retaining wall would stand up as long as its base was capable of resisting the destabilising forces. The average ϕ mobilised on plane VV controlled, to a large extent, the inclination of the resultant force acting on the base of the wall, which, in turn, significantly affected the bearing capacity of the wall base.

6. Calculations

The understanding achieved through physical modelling led to an upper-bound-like wedge method of analysis, based on the idealised failure mechanism (Mak, 1983b). The effectiveness of the method can be seen in figure 23 where the data of peak strip load are compared with calculations based on

- equilibrium consideration,
- Meyerhof's footing formula to be used for inclined and/or eccentric loads, and
- ϕ measured in the direct shear box.

7. Other System Geometries

Extending the above methodology to other system geometries, one could first ascertain the relevant collapse mechanisms by means of physical modelling, understand the mechanics involved and then establish relevant methods of analysis. Experimentally obtained peak strip loads were plotted in figure 24. Figure 25 shows the variation of the peak strip load with the distance of the footing from the wall and the length of the wall base. The wedge method could easily be adopted to cope with the effects of these two parameters. $D_F = L_H$ seemed to be the critical geometry; that was why attention was previously focussed on test C2.

8. Conclusions

The method of centrifugal modelling provides an effective way of studying the limit states of an interaction problem, thus bypassing some of the difficulties of full scale field testing. However, direct prototype modelling in the centrifuge is often problematic. The approach adopted herein was to treat the centrifuge model as an independent geotechnical event. Insights regarding the mechanics of an interaction problem were then developed by back-analysing the centrifuge model. The environment in the centrifuge lends itself to careful instrumentation, which made it possible to study the soil-structure system as an integral whole, due respect being paid to the interaction among components of the system. The usefulness of the centrifuge in encouraging and validating simple design methods has also been illustrated.

References

BOLTON, M. D. (1981) "Limit state design in geotechnical engineering", Ground Engineering Vol. 14, No. 6, 39-46.

BRANSBY, P. L. (1973) "Cambridge stress transducers", Lecture notes CUED/C-SOILS/LN2, Cambridge University Engineering Department

HAMBLY, E. C. (1969) "Plane strain behaviour of soft clay", Ph D Thesis, Cambridge University.

HANSON, J. B. (1961) "A general formula for bearing capacity", Danish Geotechn. Inst. Bull., 11.

JAMES, R. G. (1965) "Stress and strain fields in sand", Ph.D Thesis, Cambridge University.

MAK, K. W. (1983a) "Some centrifugal test results on the grain size effect in physical modelling", Technical Report CUED/D-SOILS/TR140, Cambridge University.

MAK, K. W. (1983b) "Modelling the effects of a strip load behind rigid retaining walls", Forthcoming Ph D Thesis, Cambridge University.

MEYERHOF, G. G. (1953) "The bearing capacity of foundations under eccentric and inclined loads", Proc., 3rd ICSMFE,Vol. 1, 440-445.

SCHOFIELD, A. N. (1980) "Cambridge geotechnical centrifuge operations", Géotechnique 30, No. 3, 227-268.

SCHOFIELD, A. N. (1981) "Dynamic and earthquake geotechnical centrifuge modelling" State of Art Review, Int. Conf. on Recent Advances in Geotechnical Earthquake Engineering and Soil Dynamics, St. Louis.

STROUD, M. D. (1971) "The behaviour of sand at low stress levels in the simple shear apparatus", Ph. D. Thesis, Cambridge University.

WEILER, Jr, W. A. and KULHAWY, F. H. (1982) "Factors affecting stress cell measurements in soil", J., Geo. Engng. Divn., Proc., ASCE, Vol. 108, No. GT 12, 1529-1548.

WROTH, C. P. (1975) "In situ measurement of initial stresses and deformation characteristics", Proc., Specialty Conf. on In Situ Measurement of Soil Properties, ASCE/Raleigh, N.C., 181-230.

ACKNOWLEDGEMENT

K. W. Mak wishes to acknowledge the Hackett Studentship, administered by the University of Western Australia, for financial support.

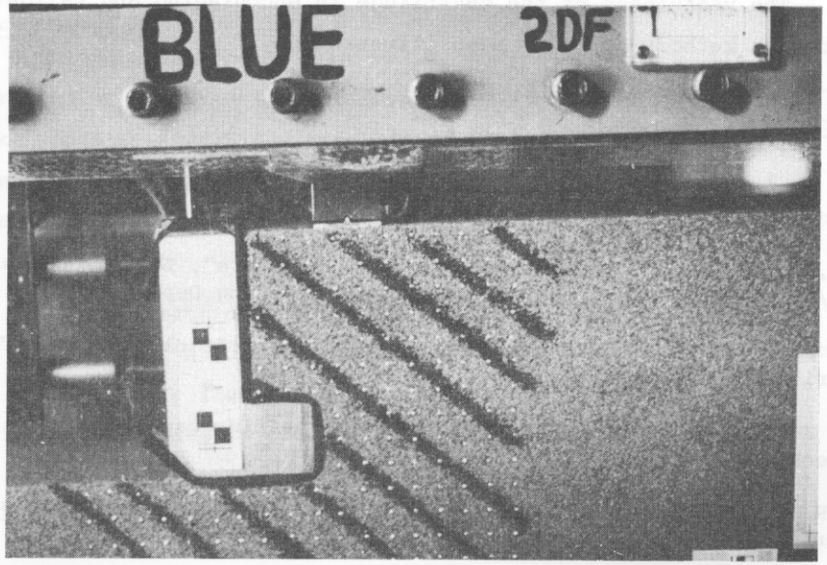

PLATE 1. A FRONT VIEW OF THE SAMPLE BEFORE THE START OF TEST C2

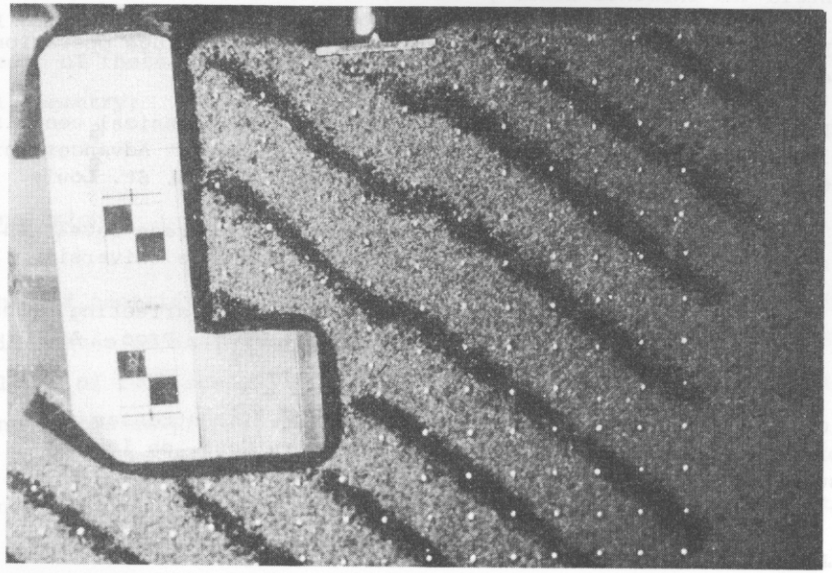

PLATE 2. FAILURE MECHANISM, TEST C2

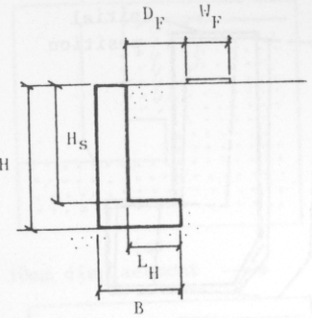

Fig. 1

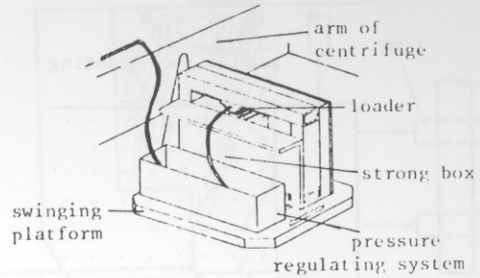

Fig. 2

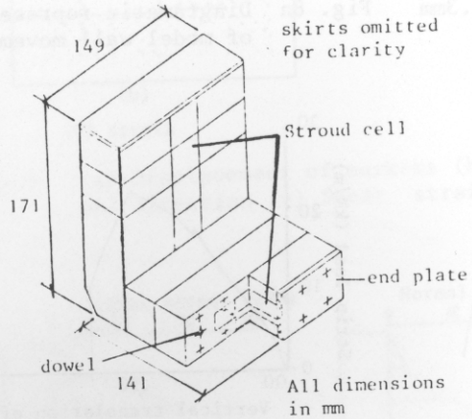

Fig. 3

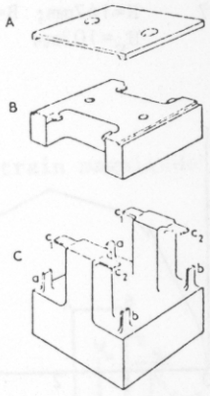

Fig. 4

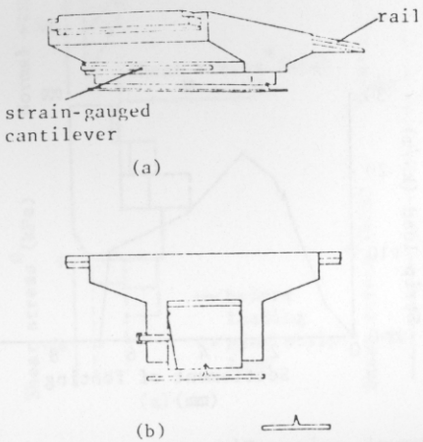

Fig. 5

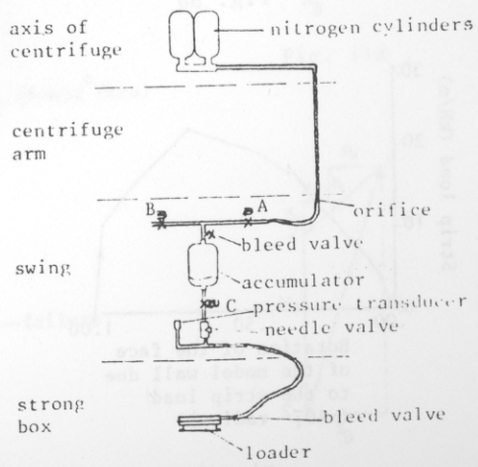

Fig. 6

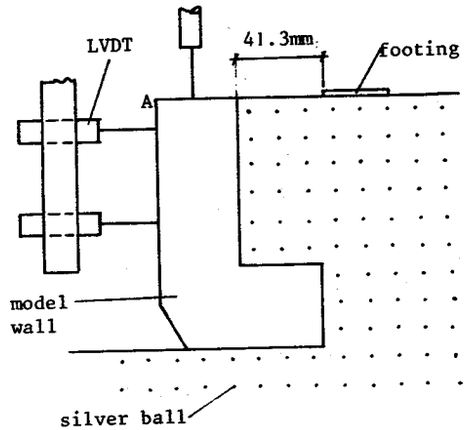

Fig. 7 H=147mm; B=74.6mm; L_H=41.3mm H_S=103mm

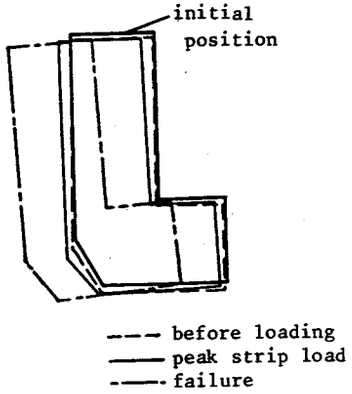

Fig. 8a Diagramatic representation of model wall movement

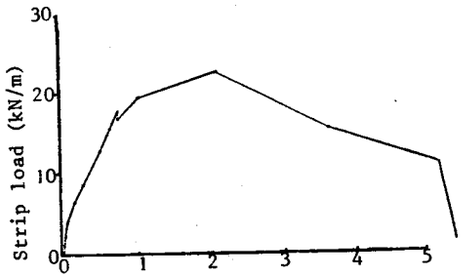

Fig. 8b

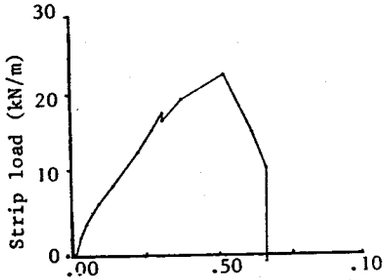

Fig. 8c

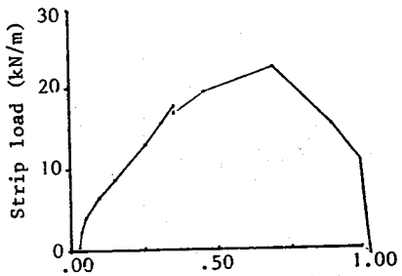

Fig. 8d

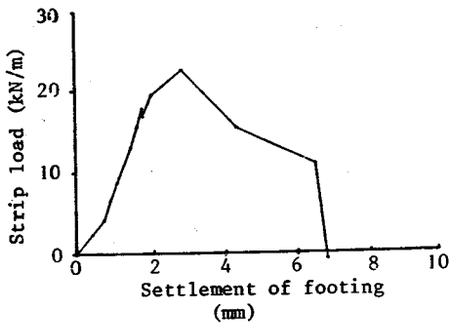

Fig. 8e

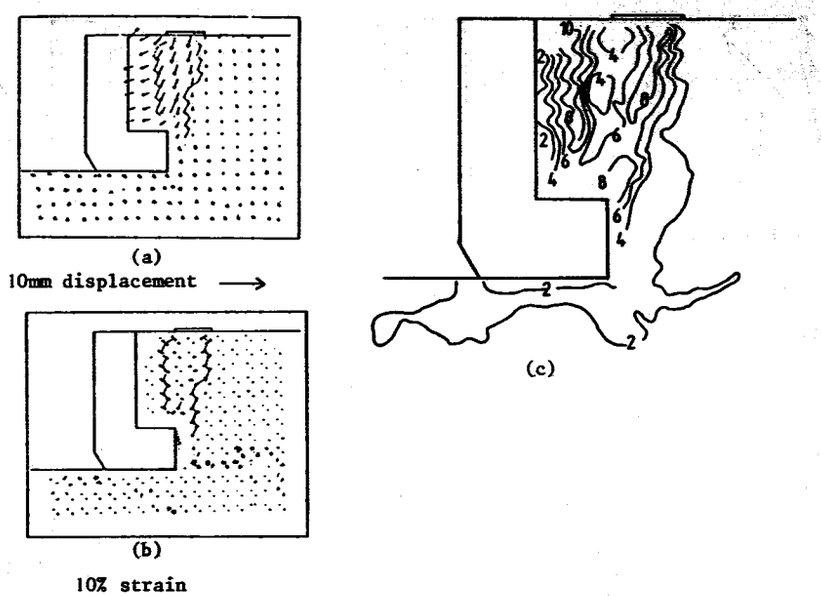

Fig. 9 (a) Displacement of markers (b) Principal strain magnitude and direction (c) Shear strain (%)

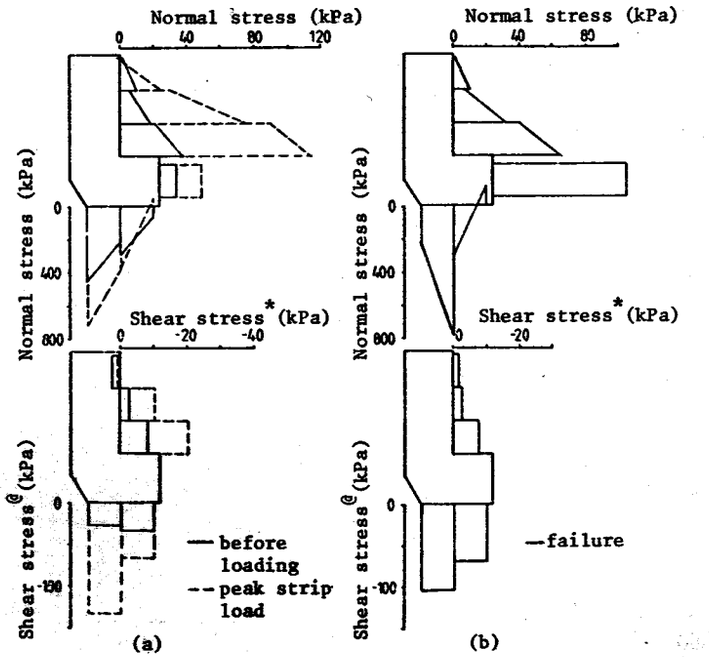

Fig. 10 * negative downward
@ negative towards the backfill

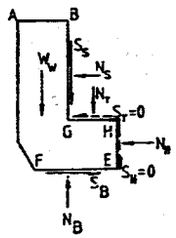

Fig. 11a

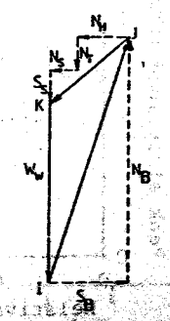

Fig. 11b

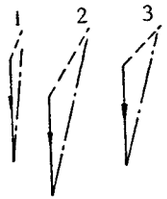

1 before loading
2 peak strip load
3 failure

Fig. 12

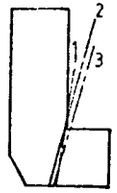

1 before loading
2 peak strip load
3 failure

Fig. 13

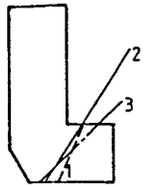

1 before loading
2 peak strip load
3 failure

Fig. 14

IP: initial position; – – –before loading; —— peak strip load; ——— failure

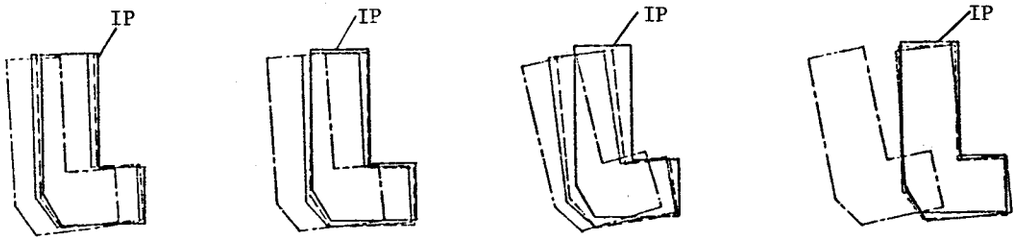

(a) Test C1 (b) Test C2 (c) Test C3 (d) Test C4

Fig. 15 Diagramatic representation of the model wall movement induced by the applied strip load. Details of the voids ratio are shown in figure 16.

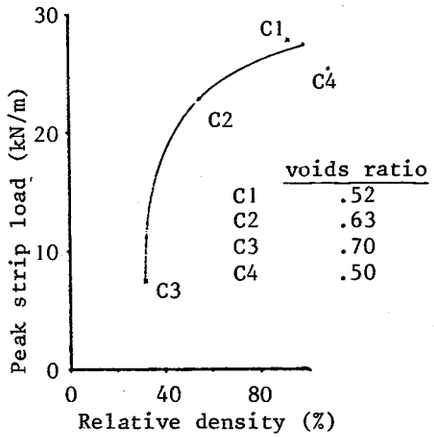

Fig. 16

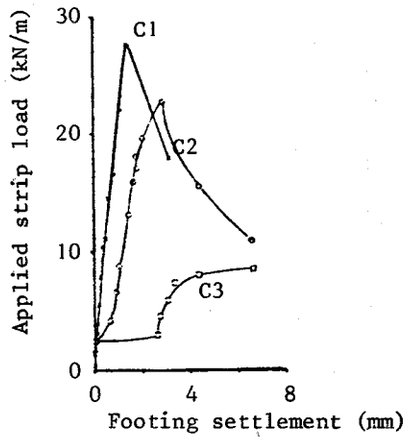

Fig. 17

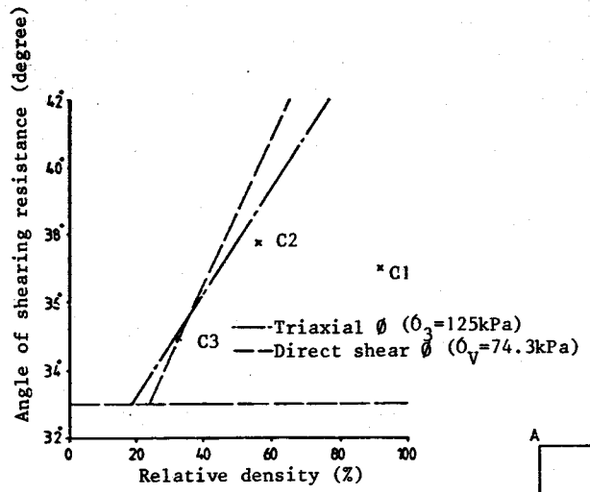

Fig. 18

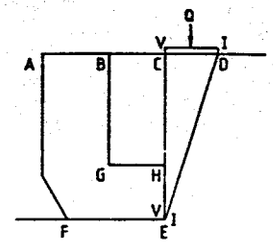

Fig. 19a

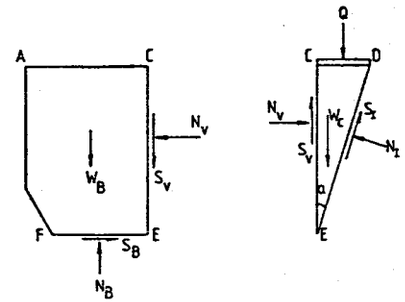

Fig. 19b

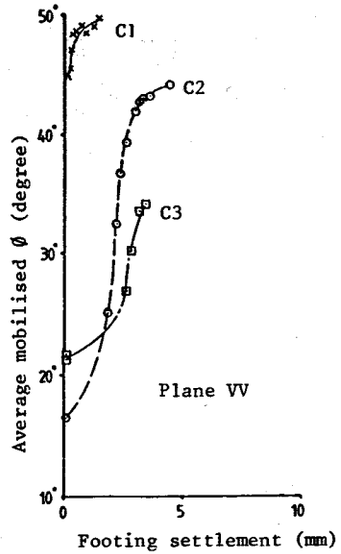

Fig. 20

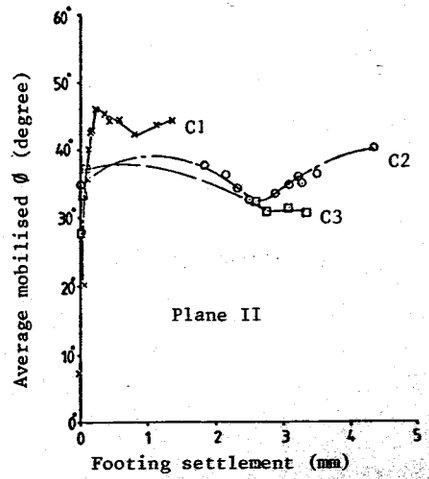

Fig. 21

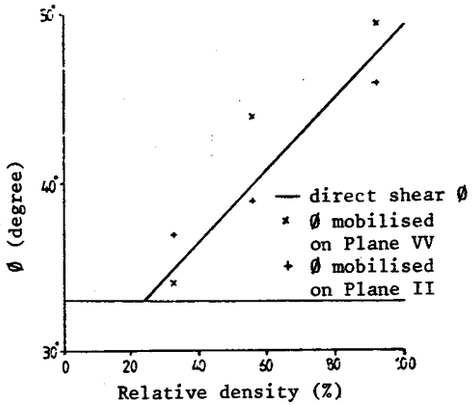

Fig. 22

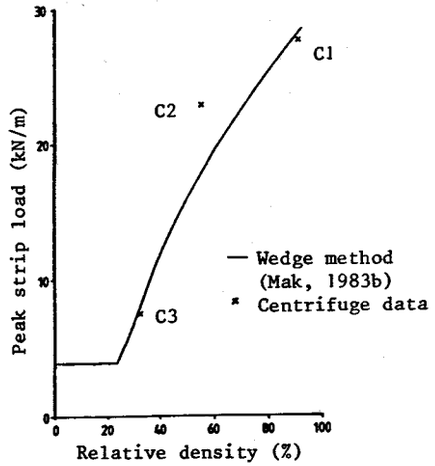

Fig. 23

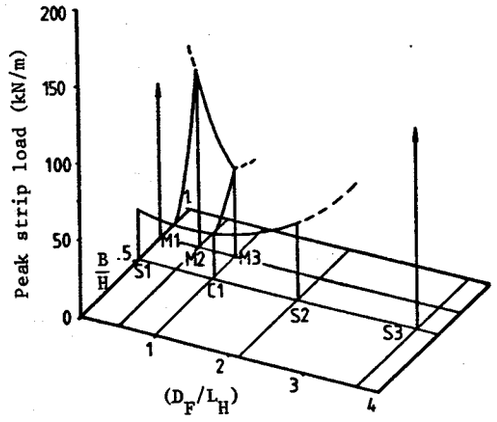

Fig. 24

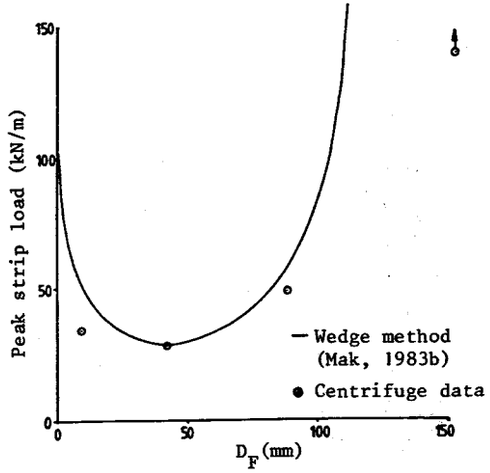

Fig. 25a

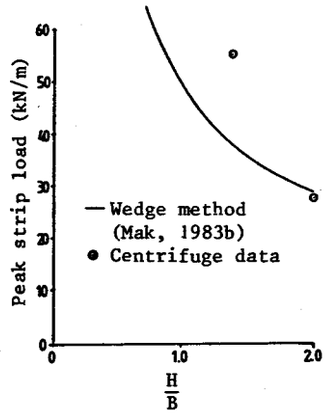

Fig. 25b